Possible formation of ancient crust on Mars through magma ocean processes

Linda T. Elkins-Tanton, Paul C. Hess, and E. M. Parmentier
Department of Geological Sciences, Brown University, Providence, Rhode Island, USA

Received 2 May 2005; revised 20 July 2005; accepted 28 July 2005; published 12 October 2005.

[1] Models for Martian magma oceans of varying depths predict that decompression mantle melting, perhaps forming Mars' earliest crust, could occur during gravitationally driven solid-state overturn of cumulates following magma ocean solidification. When hot cumulates rise from depth during solid-state overturn, some regions melt adiabatically, producing basaltic to andesitic magmas. The resulting crust would be formed at between 30 and 50 Myr after planetary accretion, when magma ocean solidification and subsequent overturn are complete. Models of magma oceans deeper than ~1550 km consistently produce two separate magmatic source regions during overturn that create compositionally distinct magmas, consistent with both major and trace element data for SNC meteorites and the Martian crust. In a partial magma ocean between ~1550 and ~1250 km (~15 GPa) the only early magma produced is from a shallow pyroxene + olivine source; but if the magma ocean were less than ~1150 km (~14 GPa) deep, the underlying (undifferentiated or minimally differentiated) mantle rises sufficiently during overturn that it melts adiabatically and produces an early magma. Magma ocean models therefore produce specific predictions for the volumes and compositions of the most ancient crust produced by a range of initial magma ocean depths. The predicted crustal compositions and volumes for a whole mantle magma ocean are consistent with observations of Mars today.

Citation: Elkins-Tanton, L. T., P. C. Hess, and E. M. Parmentier (2005), Possible formation of ancient crust on Mars through magma ocean processes, *J. Geophys. Res.*, *110*, E12S01, doi:10.1029/2005JE002480.

1. Introduction

[2] Crater densities on Mars indicate that both the southern and northern highlands date from the early Noachian [*Frey et al.*, 2002]. This ancient crust, likely formed within the first few tens or hundreds of millions of years after accretion, contains the most strongly magnetized regions on Mars [*Acuña et al.*, 1999; *Purucker et al.*, 2000]. While on the Moon the process of magma ocean crystallization and evolution is often thought to be responsible for the formation of the ancient plagioclase-rich highlands [*Warren*, 1985], perhaps the Moon's earliest surviving crust, no such anorthositic element has yet been found on Mars.

[3] The Moon is a completely dry body probably formed from heated material following the giant impact with the Earth [*Hartman and Davis*, 1975]. Its shallow pressure range and dry magma ocean composition increase the stability range of plagioclase and therefore favor formation of anorthositic crust. Mars is known to have been a wetter planet in its past, and its high mantle iron content indicates more oxidizing conditions during formation than were present on the Moon or perhaps even on the Earth, consistent with a wetter mantle. Water in silicate melt suppresses the formation of plagioclase. Fractional solidification of a deep magma ocean in a larger planet like Mars may also sequester aluminum at depth in dense majorite and garnet phases [*Hess and Parmentier*, 2001; *Elkins-Tanton et al.*, 2003a; *Borg and Draper*, 2003; *Agee and Draper*, 2004], significantly reducing the amount of aluminum available for later plagioclase crystallization [*Elkins-Tanton et al.*, 2003a, Figure 8]. The pressure of plagioclase stability is far shallower on the larger Mars than it is on the Moon, limiting the depth of crystallization over which plagioclase could float, and lessening the likelihood of floating because of the high crystal fraction at the end of crystallization. Therefore a number of reasons may be invoked to explain why a Martian magma ocean would not produce anorthosite in the quantities present on the Moon.

[4] Sources of energy to create a magma ocean on the early planet include accretion, short-lived radioisotopes, and core formation. The conversion of kinetic energy to heat during accretion may produce about 4×10^{30} J [e.g., *Wetherill*, 1990]. Accretion may happen within $\sim 10^5$ years for a Mars-sized planet [*Wetherill and Inaba*, 2000]. Among the short-lived radionuclides, ^{26}Al contributes the most heat. Assuming that ^{26}Al was created simultaneously with the solar nebula, between 10^5 years (by which time Mars may have been accreted) and the effective death of the nuclide ^{26}Al would contribute about 2×10^{30} J of energy to a planet the size and composition of Mars, sufficient in itself to melt the planet entirely. The potential energy release by core

0148-0227/05/2005JE002480$09.00

formation in Mars is expected to raise the average temperature of the planetary interior by an additional 300°C [*Solomon*, 1979]. To melt Mars approximately 2×10^{30} J are required for temperature rise to above the liquidus in addition to the heat of fusion. Therefore the sources of energy available provide many times that necessary value for melting [see also *Wood et al.*, 1970; *Solomon*, 1979; *Wetherill*, 1990], but formation of a magma ocean is also the result of a competition between energy input and radiational cooling to space.

[5] If the processes occur quickly enough or in the presence of an insulating atmosphere [*Abe*, 1993, 1997] then a magma ocean of some depth is the expected outcome. Core formation is supposed to largely or entirely postdate accretion, and may also require a magma ocean [e.g., *Jacobsen*, 2005]. Sinking of iron-rich liquids by porous flow through a silicate mantle requires interconnectivity of pore space [*Stevenson*, 1990]. Recent work by *Terasaki et al.* [2005] shows that in iron-rich Martian mantle high dihedral angles prevent percolation of iron-rich core material at pressures above 3 GPa. Core formation through a solid mantle, they conclude, is impossible; to form a core requires a magma ocean. The timing of core formation is therefore an upper bound on the completion of accretion, melting, and core formation. Over the last decade estimates based on ^{182}W anomalies for the time by which core formation of the terrestrial planets was complete has shortened from within 10 to 13 Myr [*Blichert-Toft et al.*, 1999; *Shih et al.*, 1999; *Kleine et al.*, 2002], and for Mars, to less than 10 Myr after solar system formation [*Yin et al.*, 2002; *Jacobsen*, 2005]. This short interval for core formation, alone, probably demands the existence of a molten or partially molten mantle. The existence of a large magma ocean provides important constraints to the early evolution of the Martian mantle.

[6] Fractional magma ocean crystallization produces a solid cumulate stratigraphy with an unstable density gradient, as described below. This unstable mantle overturns to a stable stratigraphy via solid-state Rayleigh-Taylor instabilities. The final materials to crystallize in this fractional process are both iron- and incompatible element-rich. They are also denser than earlier-crystallized mantle materials and therefore during gravitational overturn they sink to depth. On the Moon the sinking of late-stage iron- and titanium-rich cumulates may create a source region of a composition suitable for generating high-titanium mare basalts and picritic glasses [e.g., *Ringwood and Kesson*, 1976; *Snyder et al.*, 1992; *Hess and Parmentier*, 1995]. On the Earth, such very dense mantle materials might sink to the core-mantle boundary. This may be the origin of the deep enriched layer postulated by *Kellogg et al.* [1999], and could form the mantle reservoir containing the ^{142}Nd that appears to be missing from the portions of the mantle sampled by mid-ocean ridge and ocean island basalt volcanism [*Boyet and Carlson*, 2005]. On Mars, radiogenic heating in dense, iron- and incompatible element-rich mantle material may be the source of long-lived volcanism in the Tharsis region. This hypothesis avoids the embarrassment of having to generate Tharsis volcanism from a mantle plume that results from cooling of the core, since core cooling should be responsible for the generation of a magmatic field but none is present.

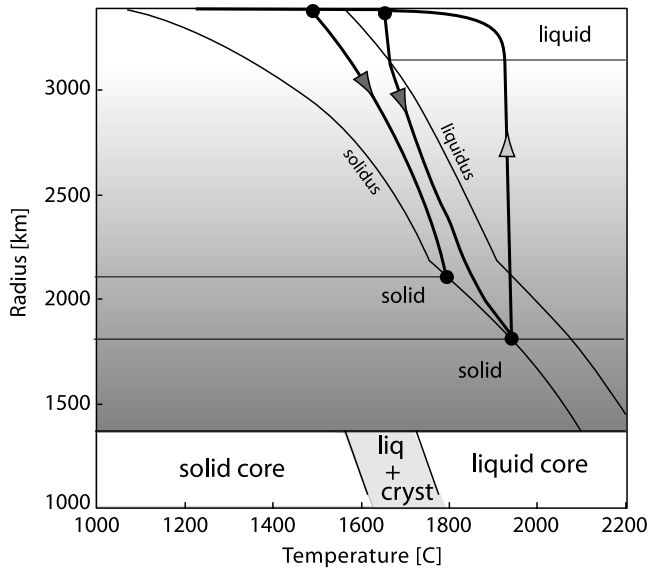

Figure 1. Solidus and liquidus for Martian core and mantle from *Longhi et al.* [1992] in thin solid lines, with idealized paths of convecting magma ocean liquids in P-T space. A hot upwelling path is shown on the right, along with two possible downwelling paths. The first downwelling begins in an entirely liquid region of the top boundary layer and through heat of fusion sinks to a similar temperature as the initial hot upwelling. The second downwelling begins in a colder region of the top boundary layer and becomes completely solid before reaching the depth of the initial hot upwelling. Downwelling and upwelling regions therefore may create topography at the bottom of the solidifying magma ocean.

[7] While dense cumulates from the near-surface sink during overturn, hot cumulates from the deep mantle rise to gravitational stability near the surface, and may melt adiabatically, producing the earliest crust. In this paper we present model predictions for the compositions and volumes of this earliest crust, and compare them with available data from Mars. We regard fractional solidification and overturn as an idealization that produces extreme ranges of composition in the resulting solid mantle. Therefore the predictions presented in this model reproduce the ranges of Martian compositions but should not be used to interpret the petrogenesis of each individual Martian meteorite. In addition, the processes of assimilation and fractional crystallization that certainly affected the composition of crustal rocks, including the meteorites, are not considered in this paper.

2. A Stagnant Lid on a Magma Ocean Is Unlikely

[8] The fundamental processes within a crystallizing magma ocean are summarized by *Solomatov* [2000] and discussed in detail for Mars by *Elkins-Tanton et al.* [2005]. In summary, vigorous convection in the low viscosity liquid magma ocean is assumed to maintain a homogeneous liquid composition and an adiabatic variation of temperature with depth. Because adiabats are steeper than solidii, a solid region develops at the bottom of the mantle and thickens as the ocean cools (Figure 1). During the rapid solidification of

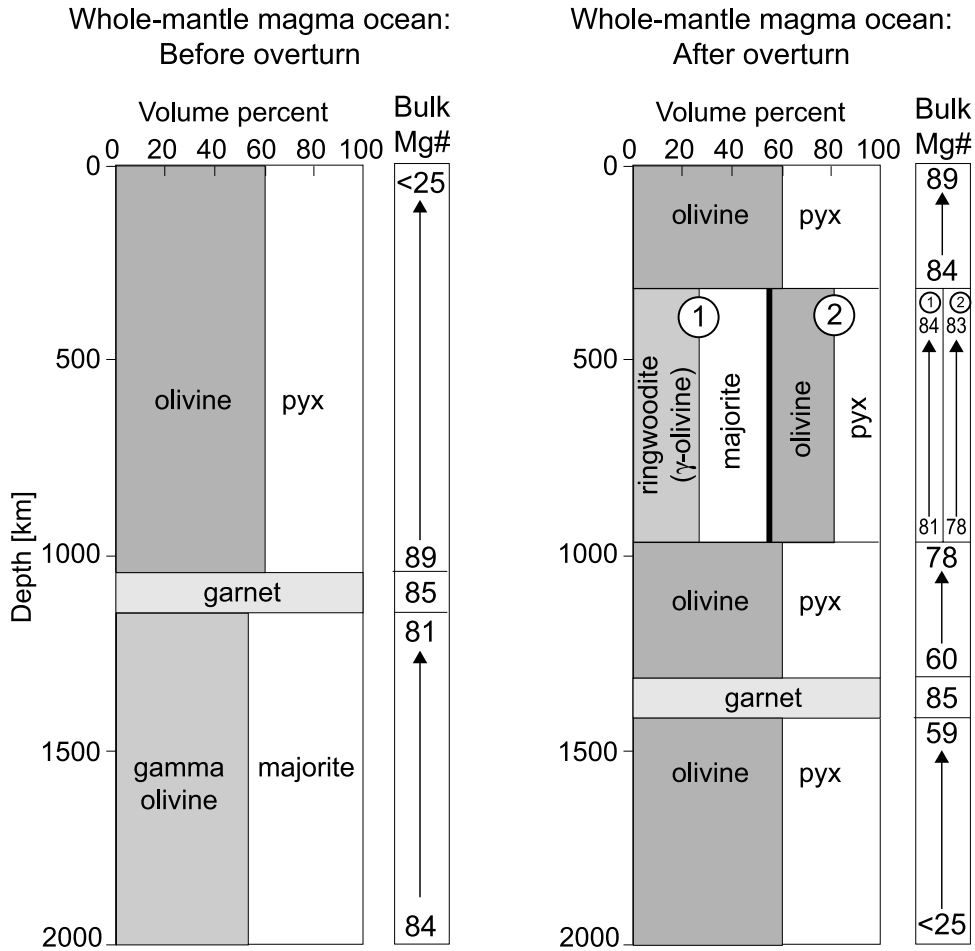

Figure 2. (left) Solidified mantle mineralogy follows the bulk mantle composition given by *Bertka and Fei* [1997] with simplified phase relations from *Longhi et al.* [1992]. In this example, the magma ocean is assumed to be 2000 km deep above a core with radius 1396 km (24 GPa) [*Bertka and Fei*, 1998], and garnet is assumed to settle into a concentrated layer. (right) Stratigraphy following solid-state overturn of a whole mantle magma ocean, with the upper mantle heterogeneous region marked. Mg numbers given (where Mg# = molar(Mg/(Mg + Fe))) are for the bulk material.

a magma ocean, cumulates are assumed to retain their solidus temperatures and compositions.

[9] The majority of the magma ocean is predicted to solidify over a period on the order of 10^5 years, though the remainder of the magma ocean may not be completely solidified for an additional 20 Myr [*Abe*, 1997; *Tonks and Melosh*, 1990]. During solidification the formation of a stagnant conductive lid on the magma ocean is unlikely. *Abe* [1997] estimated that a water atmosphere may provide sufficient insulation to maintain the magma ocean in a completely liquid state at its surface. In the absence of such insulation, the surface of the magma ocean will quench to solid against the cold of near-space or a thin atmosphere. Once solidified, the material in the lid will be denser than the liquids beneath. The lid will be prone to foundering through its own weight, convective stresses on its bottom boundary, and disruption by impacts. On terrestrial magma pools solid crusts may persist through support at the edges of the pool, but on a planetary magma ocean gravitational forces dominate and any solid lid should founder. *Walker and Kiefer* [1985] considered the ramifications of cold foundering material in a lunar magma ocean, and found that even meter-sized pieces of cooled, solidified material may sink to the bottom of the magma ocean. These foundering pieces cool the magma ocean from its bottom, speeding its crystallization, and possibly ameliorate the effects of fractionation through their primitive bulk compositions.

3. Compositional Heterogeneity in the Solidified Magma Ocean

[10] The completed cumulate stratigraphy from fractional solidification (Figure 2) results in an unstable density stratification, primarily because of magnesium and iron exchange within the evolving magma ocean liquids. A gravitationally unstable stratigraphy will overturn via Rayleigh-Taylor instabilities to a stable profile with intrinsically densest materials at the bottom, on timescales that depend on the rate of thermally activated creep [*Solomatov*, 2000; *Elkins-Tanton et al.*, 2003a].

[11] A possible exception to overturn is a hypothetical topmost layer of the solidified magma ocean: as solidification proceeds any initial water content in the magma ocean will be concentrated in the evolving liquid fraction, since

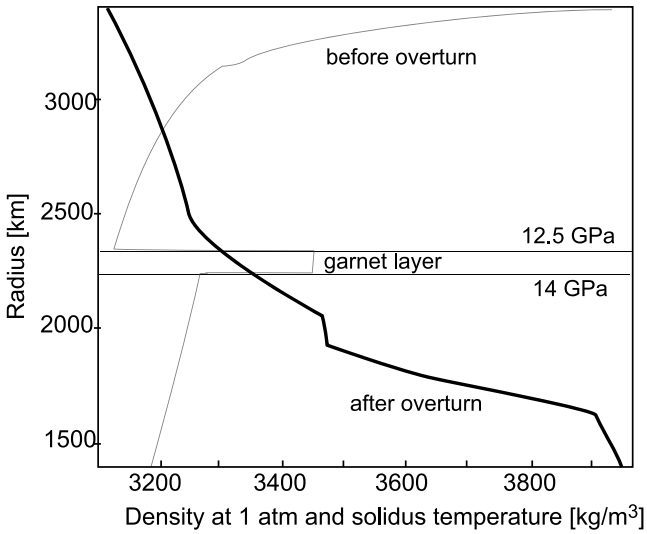

Figure 3. Pre-overturn and post-overturn density profiles for a simple fractional crystallization model of a whole mantle Martian magma ocean showing the gravitational stability of the mantle after overturn, and the existence of overlapping density gradients before overturn that result in lateral compositional and temperature heterogeneities in the overturned mantle.

the magma ocean will be crystallizing nominally anhydrous mineral phases [*Ohtani et al.*, 2004]. The last fraction of solidification will occur near the planetary surface in the presence of a high crystal fraction and water content equivalent to about one quarter of the initial magma ocean water budget [*Elkins-Tanton and Parmentier*, 2005]. The topmost crystallizing layer is likely to be silica-rich and therefore portions may be buoyant, though any mafic minerals will be highly iron-enriched and therefore dense (note that this may be an ideal formation scenario for Martian meteorite ALH84001, an ancient orthopyroxenite requiring an alumina-poor, low-pressure provenance). Since this buoyant layer is nearest the surface, it is the coldest and therefore stiffest layer. Though numerical modeling indicates that virtually the entire magma ocean participates in overturn, portions of the final layer that are buoyant and hydrous have the greatest chance of remaining in place. There may exist on Mars therefore limited remnants of a hydrous stagnant lid, buried under the voluminous basaltic melts discussed in this paper, though possibly visible in the deepest craters. Indeed, this early material might be a reservoir of highly incompatible elements on Mars, though the majority of incompatible elements are expected to participate in overturn along with the densest iron-rich mafic cumulates.

[12] Though in general the magma ocean cumulates increase in density with radius, solidification models indicate that cumulates do not form a monotonic density gradient: the pre-overturn profile in Figure 3 clearly shows that cumulates in portions of the lower and upper mantle have identical densities but with different bulk compositions and correspondingly different mineralogies. Numerical models indicate that non-monotonic density profiles overturn to form mantles that are laterally heterogeneous compositionally [*Zaranek et al.*, 2004; *Elkins-Tanton et al.*, 2005]. The density structure in these models approaches a final state after overturn of a purely radial density stratification decreasing monotonically with radius. The densest materials from near the surface have sunk to the core-mantle boundary and buoyant mid-mantle material has risen to the surface. Upgoing and downgoing plumes, however, have stalled at neutral buoyancy, creating a radius interval containing large-scale lateral heterogeneity in temperature, mantle composition and concentrations of radiogenic and trace elements. This lateral heterogeneity has implications for magmatic source regions as well as the initiation and pattern of thermal convection, and can be seen in temperature profiles in Figure 4. The final overturned cumulate stratigraphy therefore is radial in its density structure but heterogeneous laterally in composition.

[13] During overturn, hot cumulates rise from depth and may decompress above their solidii and melt, producing an early crust. No early stagnant lid is likely to form before the shallow magma ocean contains a significant crystal fraction, though the final solidifying cumulates may be too viscous and buoyant to entirely participate in overturn. Adiabatic melting during solid-state cumulate overturn following magma ocean crystallization is the likeliest process to produce the earliest crust of Mars, and would likely flood any stationary remnants of magma ocean crystallization. Simultaneously cold cumulates from near the surface sink to the core-mantle boundary, creating heat flux out of the core sufficient to drive a short-lived, strong core dynamo, consistent with the timing of magnetization measured on Mars [*Elkins-Tanton et al.*, 2005].

4. Importance of a Gravitationally Stable Mantle

[14] Overturn reorders the mantle layers into a configuration that is gravitationally stable. An early planet envisioned as hot and active has been assumed to convect vigorously [e.g., *Schubert and Spohn*, 1990]. Stable compositional stratification after overturn, however, would

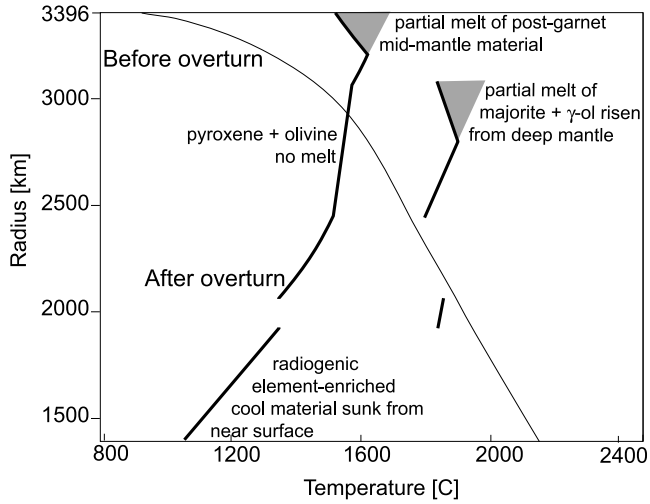

Figure 4. Post-overturn temperature profiles for the model shown in Figures 2 and 3 showing regions of adiabatic melting during overturn. In the shallower melting region the melt fraction approaches 60% at its shallowest point, and in the deeper melting region melting approaches 50%.

inhibit thermally driven convection due to cooling at the surface or heating at the core mantle boundary [*Zaranek and Parmentier*, 2004]. If thermally driven convection is inhibited by the stable mantle configuration after overturn, the deepest layers of the mantle will be difficult to mobilize for later adiabatic melting, and products derived from them may seldom or never been seen at the planet's surface. Radiogenic elements, however, are generally incompatible and are concentrated in the final shallow crystallizing cumulates. The final cumulates largely sink during overturn to the core-mantle boundary, though some portions may remain in place, not participating in overturn. Over time radiogenic heating in the evolved fractions, particularly those in the deep mantle, could cause in-situ thermal convection or even melting.

[15] The SNC meteorites contain compositional evidence for the formation of isotopically distinct mantle source regions that formed in the first few tens to hundreds of millions of years on Mars [*Jones*, 1986; *Borg et al.*, 1997, 2002]. The wide range of the Martian ε^{Nd} values far surpasses terrestrial values, and the presence of ^{142}Nd anomalies indicate the SNC source reservoirs differentiated very early and have remained separate up through the most recent magmatism that produced the SNC meteorite material [*Shih et al.*, 1982; *Jones*, 1986; *Harper et al.*, 1995; *Borg et al.*, 1997; *Brandon et al.*, 2000]. Magma ocean solidification processes provide a means to create compositionally distinct mantle reservoirs early in planetary evolution [*Elkins-Tanton et al.*, 2003a] that are preserved by their stable density profile that inhibits vigorous thermal convection. Magma ocean processes therefore are consistent with the formation of Mars' earliest crust and magnetic field, and with the creation and preservations of SNC mantle source reservoirs.

5. Model

[16] The models for magma ocean crystallization, gravitational overturn with simultaneous adiabatic melting and creation of an early magnetic field are described in detail by *Elkins-Tanton et al.* [2003a, 2005]. These models use the bulk Martian silicate composition given by *Bertka and Fei* [1998] and the solidus and liquidus of *Longhi et al.* [1992]. Calculating trace element and isotopic compositions of cumulates and subsequent melts is critical to allow comparison with Martian data. The distribution of incompatible elements during solidification, in particular heat-producing U, Th, and K, depends highly on the presence of even small amounts of melt retained within solidifying regions. Melt retention will in turn depend on the relative rates of melt migration and compaction of the mostly solid mantle, an aspect of the model under current consideration. The models incorporate interstitial melt and trace element partitioning using the coefficients from *Draper et al.* [2003] and *Green et al.* [2000] (Table 1) and varying the trapped melt fraction, and Sm/Nd and Lu/Hf ratios and initial isotopic compositions for each layer of the crystallizing magma ocean are calculated.

[17] Crystallization is expected to occur in cold, mostly liquid downwellings that impinge on the top of previously solidified cumulates. At sufficiently high pressure olivine and pyroxene are more buoyant than coexisting liquids [*Stolper et al.*, 1981]. In our models the depth of neutral buoyancy for olivine and pyroxene occurs at 7.5 GPa; however, garnet is negatively buoyant at all pressures. Dense garnet crystals may then settle while olivine and pyroxene remain suspended in the convecting liquid. Segregation of the dense garnet depends on the relative rates of settling and reentrainment by return flow near the boundary with underlying solids [*Martin and Nokes*, 1989; *Tonks and Melosh*, 1990].

Table 1. Partition Coefficients Used in Calculating Cumulate and Liquid Compositions in a Fractionally Crystallized Magma Ocean[a]

Mineral	Sm	Nd	Lu	Hf
Majorite[b]	0.2	0.07	3.5	0.5
Ringwoodite (γ olivine)[c]	0.0006	0.0001	0.02	0.01
Garnet[b]	3	0.05	6	0.4
Clinopyroxene[d,e]	0.2	0.1	0.3	0.2
Orthopyroxene[d,e]	0.02	0.02	0.03	0.05
Olivine[d]	0.0006	0.0001	0.02	0.013

[a]Partition coefficients are wt% in solid/wt% in liquid.
[b]*Draper et al.* [2003, and references therein].
[c]Ringwoodite is assumed to have partition coefficients similar to olivine.
[d]*Snyder et al.* [1992].

[18] In the simple models presented here, garnet settles to form a ~150 km-thick layer beginning at 14 GPa. Following garnet segregation pyroxene and olivine continue to crystallize, but remain suspended in the magma ocean within the pressure interval between the top of the garnet layer and the end of their positive buoyancy at ~7.5 GPa. Magma ocean cooling and crystallization will continue until a critical crystal fraction is obtained at which solids form a resilient network. Pore fluid convection through the network, however, may continue to reequilibrate the solid phases. In the largely liquid region above the network, olivine and pyroxene crystals are no longer buoyant and will settle to the new bottom boundary layer at 7.5 GPa. A likely outcome of this process is effective batch crystallization of pyroxene and olivine within the network in the pressure interval from the top of the garnet layer to 7.5 GPa, while the rest of the magma ocean evolves by fractional crystallization.

[19] Following solidification the unstable cumulate mantle overturns via Rayleigh-Taylor instabilities to a gravitationally stable stratigraphy (densities are calculated using a database of pressure-, temperature-, and composition-dependent thermochemical parameters), and the models predict the movement and final stable positions of the cumulates, while tracking temperature, density, major and trace element composition, and mineralogy. These parameters allow calculation of possible core dynamos [*Elkins-Tanton et al.*, 2005], as well as the time of onset of thermal convection as cooling of the stably stratified overturned cumulates proceeds [*Elkins-Tanton et al.*, 2003a]. The compositions and temperatures of cumulates rising during overturn are used to calculate any resulting adiabatic melting, using the MELTS program [*Ghiorso and Sack*, 1995].

6. Results

[20] The earliest planetary crust in our models forms from adiabatic melting of hot cumulates that rise above their

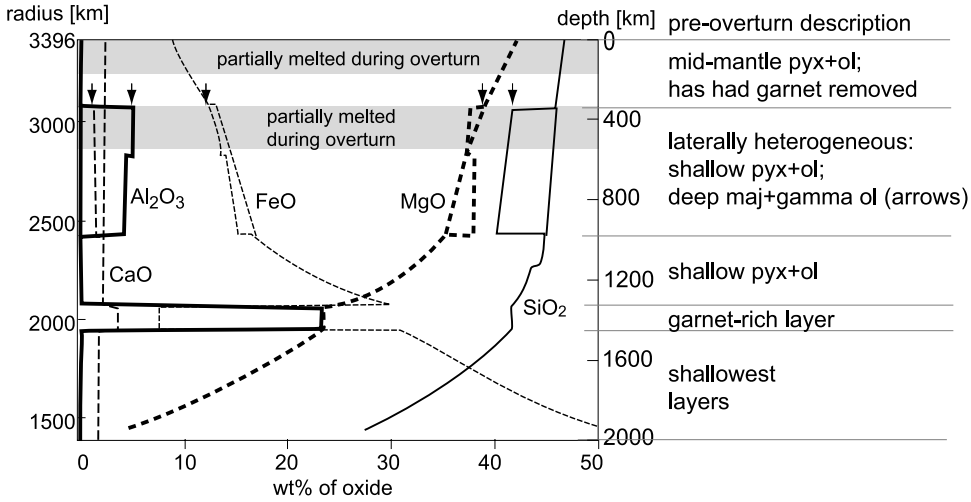

Figure 5. Post-overturn major element oxide compositions in the Martian mantle, showing regions of partial melt from adiabatic ascent during overturn. Regions of melt correspond to those marked in Figure 4 and result in the magmas posited for crustal formation. The deeper melting zone consists of materials intruded in the solid state from depth, creating a laterally heterogeneous mantle over the depth range shown. The composition that melts (marked with arrows) will not therefore lie in a concentric layer, but be distributed as regions in some pattern around the mantle that corresponds to its spherical harmonic mode of overturn. A description of the cumulates' pre-overturn position and mineralogy is given on the right.

solidii during solid-state overturn. In the models with a full-mantle magma ocean two distinct regions of the cumulate mantle melt to form the earliest crust, while in shallower magma oceans the melting regions depend upon the depth of the magma ocean, as described below. In contrast to evidence from the Moon, on Mars highly incompatible-element enriched and radiogenic compositions may be carried to depth during overturn and may only possibly appear in later volcanic events, though some may remain near the surface in some fraction of the possibly buoyant and stiff felsic end of magma ocean crystallization.

6.1. Magma Production During Solid-State Overturn: A Whole Mantle Magma Ocean

[21] Two mantle source regions melt during solid-state overturn to form the earliest crust in Martian full-mantle magma ocean models (Figures 4 and 5). The shallowest source is olivine + pyroxene cumulates at about 1600°C that rise from the mid-mantle just above the garnet layer to near the surface, forming a layer from the surface to a depth of about 200 km (Figure 2, right). This source has an initial $^{147}Sm/^{144}Nd$ ratio of ~0.20, Mg#s (defined as molar Mg/[Mg + Fe]) from 87 to 89, Al_2O_3 content on the percent level, and SiO_2 of about 46%.

[22] Beneath this shallowest melting olivine + pyroxene layer a laterally heterogeneous mantle forms during overturn over a radius interval from ~300 to 950 km depth. One olivine + pyroxene assemblage remains approximately where it originated (between about 600 and 200 km depth) and therefore will not melt adiabatically. A second assemblage consisting of majorite + ringwoodite (γ-olivine) converted to garnet + pyroxene + olivine (bulk composition indicated by arrows in Figure 5) at potential temperatures between 1800 and 2000°C rises from depth to intrude the nearly stationary olivine + pyroxene cumulates (Figure 2, right). These deep cumulates cease rising when their buoyancy is neutral, producing a mantle laterally heterogeneous in temperature and in composition. Compared to the shallower melting source, they have higher initial $^{147}Sm/^{144}Nd$ ratios, in places as high as 0.6, Mg#s of about 81 to 85, Al_2O_3 content of about 5%, and SiO_2 of about 42%.

[23] Starting with the compositions of the two predicted source regions, MELTS [*Ghiorso and Sack*, 1995] is used to estimate their different solidus temperatures and the resulting melt compositions. The shallowest, olivine + pyroxene cumulates melt from 10 to 60% depending on the extent of their rise (Figures 4 and 5). The deepest of this layer to melt (smallest melting extent) lie at about 150 km depth. This shallowest source produces magmas with compositions in the range of 48 to 54% silica and Mg#s in the 70s. The deeper cumulates melt approximately 10 to 50%. The deeper cumulates that melt ~50% lie at about 300 km depth, and the melting zone extends to about 500 km depth, with melt fraction decreasing with depth. The cumulates at 300 to 500 km depth produce magmas with 45 to 56% silica, Al_2O_3 from 5 to as high as 15%, and Mg#s in the 60s.

6.2. Magma Production During Solid-State Overturn: A Shallower Magma Ocean

[24] The total energy from planetary accretion, the contributions of short-lived radionuclides, and heat from core formation is sufficient to melt the whole silicate mantle. The timing of these events and the state of insulation of the planet, however, may have allowed heat to conduct into space sufficiently that only a portion of the Martian silicate mantle melted. A range of magma ocean depths are considered, all assuming the underlying undifferentiated material has the bulk composition given by *Bertka and Fei* [1998]. The phase assemblage of this primitive mantle is assumed to be that of experiment BF-54 from *Bertka and*

Fei [1997], performed at 21 GPa and 1750°C, which contained 54% ringwoodite and 46% majorite. This layered model is a simplification of the likelier initial state where a liquid magma ocean merges into a primitive lower mantle through a partially molten zone with decreasing melt fraction.

[25] Fractional crystallization from a magma ocean necessarily creates early cumulates with lower densities (high MgO content) than the undifferentiated progenitor, and late cumulates from evolved liquids that are denser (high FeO content) than the undifferentiated material. If its viscosity is low enough to allow flow during solid-state cumulate overturn, the primitive material will rise to a level of neutral buoyancy that is at a shallower level in the Martian mantle. These models assume that the primitive mantle is just a few tens of degrees cooler than its solidus, meaning that both its viscosity and thermal buoyancy are equivalent to the cumulates resulting from magma ocean crystallization. To calculate the final level of neutral buoyancy for the primitive material, its density is recalculated stoichiometrically as the upper mantle assemblage of olivine, pyroxene, and garnet so it can be compared to shallower phase assemblages [see *Elkins-Tanton et al.*, 2003a].

[26] The whole mantle magma ocean described above produces an overturned, gravitationally stable cumulate mantle in which majorite + ringwoodite from the lower mantle has risen far enough to exceed its solidus temperature and melt adiabatically. In the stratigraphy that results from a partial magma ocean, the primitive mantle material is more buoyant than both the garnet-rich layer and the densest, final cumulates that form near the surface of the magma ocean (disregarding any hypothetical thin, final plagioclase-rich layer). During overturn, therefore, both the shallowest, dense cumulates and the garnet layer would sink through the primitive material, and the primitive material would rise to the mid-mantle. Lower mantle majorite + ringwoodite from magma ocean differentiation, however, is more buoyant than the primitive undifferentiated material. Depending upon the depth of the initial magma ocean, therefore, the possibility of adiabatically melted primitive material exists along with the possibility of melted majorite + ringwoodite differentiates.

[27] If the partial magma ocean is as deep as ~1550 km (~19 GPa) then the layer of differentiated majorite + ringwoodite that crystallizes between 19 GPa and 14 GPa (after which point garnet is stabilized) is thick enough to rise above its solidus and melt much as described in the whole mantle magma ocean above. In a partial magma ocean between ~1550 and ~1250 km (~15 GPa) deep neither the primitive material nor the majorite + ringwoodite cumulates rise sufficiently to melt. The only magma produced is from the shallowest pyroxene + olivine composition and is identical in composition to that created from the whole mantle magma ocean. If, however, the magma ocean is less than ~1150 km (~14 GPa) deep, the primitive material rises sufficiently during overturn to melt adiabatically.

[28] Far shallower magma oceans have not been modeled. Without the large volumes of majorite and garnet fractionation allowed by deep pressures, magma ocean liquids would be alumina-enriched at low pressures, stabilizing plagioclase in sufficient volumes to necessitate changing the simple mineral assemblages shown in Figure 1.

7. Discussion

[29] Magmas produced by adiabatic melting during cumulate overturn are candidates to make the oldest Martian crust. A crust produced in this manner may have persisted to the present-day on Mars, albeit partially covered by subsequent volcanism or sedimentation. Models of magma oceans deeper than ~1550 km consistently produce two separate magmatic source regions during overturn that create compositionally distinct magmas. Most models produce an identical shallow magma source region consisting of post-garnet pyroxene + olivine that melts to create low-alumina basaltic magmas. Some models have, in addition, a converted majorite + ringwoodite source region, or a region of primitive mantle material that partially melts by pressure-release.

[30] The differentiated Martian mantle predicted in these models would be an idealization of the earliest mantle on Mars. Overturn predicts melting to create the earliest crust on Mars, and the compositions of melts from the modeled source compositions are calculated using the MELTS program [*Ghiorso and Sack*, 1995], though the program was not designed for such evolved compositions and so melt compositions calculated in this way must be viewed as only approximations to the real magma compositions. The magma compositions produced by the MELTS program form a rough estimate of the parental melt compositions expected for the earliest Martian crust.

[31] The data available for comparison with modeled source regions and resulting magmas consists of SNC meteorites and mission data of crustal compositions of undetermined age from both southern and northern hemispheres. SNC meteorites and some crustal compositions are all the result of volcanic events far younger than the earliest crust-forming events predicted here. The earliest crust is expected to have been formed before 50 Myr after planetary accretion, while some SNC meteorites are as young as a few hundred million years before present.

[32] SNC meteorites and modern crustal compositions are also expected to be the result of secondary processes such as convective mixing of source regions, magma mixing, fractionation, accumulation, and assimilation. These secondary processes all change major element compositions significantly, but incompatible trace elements ratios to a far lesser degree (with the exception of assimilation or mixing, depending upon the assimilated composition). Trace element and isotopic ratios therefore make the most useful comparisons with Martian data from missions or meteorites, in the absence of significant magma mixing or assimilation, and are shown in Figures 6 and 7. Workers have also made progress toward estimating the compositions of SNC meteorite source region compositions (see references in *Borg and Draper* [2003]). The source regions of the meteorites should be most directly comparable to the predicted mantle cumulate compositions of this model, and are shown in Figure 7.

[33] Trace element comparisons between model source regions and estimates of the SNC source regions (references given in figure captions) are favorable. First, the total Lu/Hf

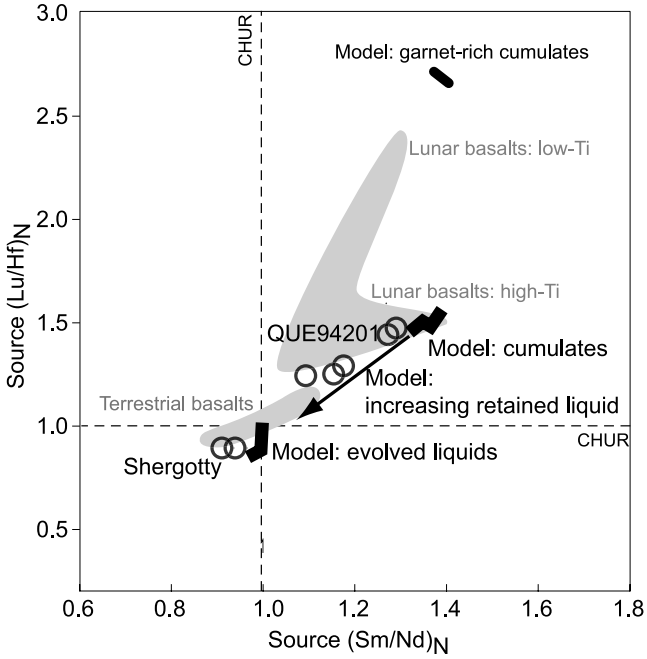

Figure 6. The initial Lu/Hf ratios of source regions for various planetary magmas are shown versus their Sm/Nd ratios, all normalized to chondritic values [*Anders and Grevesse*, 1989]. Our model results are shown in solid black, corresponding well to the SNC meteorite estimates shown as circles but differing from lunar compositions. After Figure 2 of *Blichert-Toft et al.* [1999].

and Sm/Nd ratios for modeled cumulates with intercumulus liquids closely fit SNC meteorite data and fall conspicuously far from both lunar and terrestrial magmas (Figure 6). Figure 6 shows that the SNC meteorites thought to come from depleted regions, for example QUE94201 and Chassigny, are encompassed within the mantle cumulates of this model, while those with an enriched signature (e.g., Shergotty and Zagami) [*Blichert-Toft et al.*, 1999; *Herd et al.*, 2002; *Borg et al.*, 2002] are similar in composition to the evolved liquids produced by extensive fractionation of the magma ocean.

[34] The range of $^{176}Lu/^{177}Hf$ estimated to be appropriate for the SNC meteorite source regions (0.0276 to 0.0482) correlates well with the majority of the modeled Martian cumulate mantle (0.027 to 0.028), though not with the deeper source region that originally formed as majorite + ringwoodite in the lower mantle (0.07 to 0.16) (Figure 7). *Borg and Draper* [2003] also find on the basis of analysis of the Lu and Hf contents of the SNC meteorites that shallow melting regions on Mars must come from sources that were previously depleted in garnet. Initial $^{147}Sm/^{144}Nd$ ratios for the shallow melting source are ~0.2, while the deep melting source has $^{147}Sm/^{144}Nd$ ratios as high as 0.6. The shallow source region creates melt consistent with estimates by *Longhi* [1991] and *Norman* [1999] for the initial $^{147}Sm/^{144}Nd$ of the Martian juvenile crust of between 0.15 and 0.17.

[35] Major element comparisons between modeled magmas and the SNC compositions themselves are shown in Figure 8 and show reasonable agreement with the averaged compositions for the SNC meteorites despite the wide disparity in ages of formation. Similarly composed source regions therefore may have melted throughout Martian history to produce volcanism. Melts from the shallowest melting region form reasonable matches for the most magnesian SNC compositions, while the modeled magmas from the deeper source region are far more aluminous than the majority of the SNCs.

[36] Melts from a primitive mantle, by comparison, would be tholeiitic and possess ε_{Nd} values of approximately zero. No such material has been found on Mars. The primitive mantle itself would be radiogenic compared to the majority of cumulates and would be expected to heat to the point of thermal convection and melting over the age of the planet, possibly resulting in the production of voluminous younger crustal materials, also not seen. We therefore posit that the existence of a significant primitive fraction in the Martian mantle is unlikely.

[37] The total melt volume produced during overturn of a whole mantle magma ocean would be sufficient to spread over the surface of Mars to a depth of ~100 km. These estimates are roughly double the geophysical estimates of the current Martian crust of about 50 km [*Neumann et al.*, 2004], but these estimates are probably maximum values. First, any material that did not participate in overturn may halt ascent of buoyant materials during overturn and limit their adiabatic melting. Subsequent segregation of melt from cumulates is likely to be incomplete, particularly from the deep melting region where some melts are required to migrate through 500 km of material to reach the surface. The modeled melt volumes are therefore considered roughly consistent with Martian crustal estimates.

[38] The volume of melt produced in the shallower cumulates is about twice the volume of melt produced in the deeper cumulates. The likelihood of overturn occurring in a spherical harmonic degree-one pattern [*Zhong and Zuber*, 2001] combined with the two compositions and volumes of crustal production raise the possibility of over-

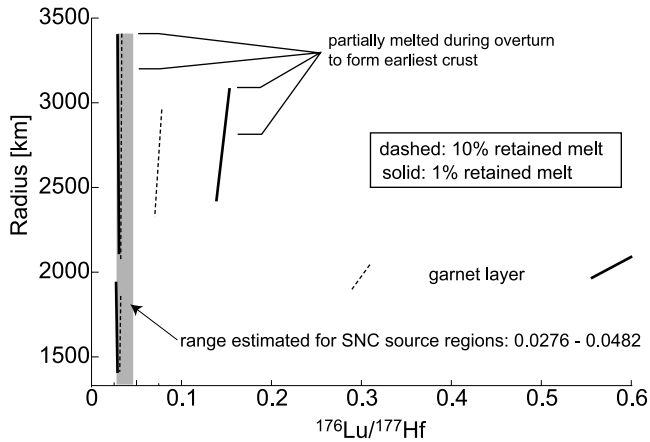

Figure 7. The radius of Mars is shown versus the initial $^{176}Lu/^{177}Hf$ ratio of the predicted Martian mantle after solid-state cumulate overturn. The regions predicted to melt to form the earliest crust are shown in black brackets, and the range of $^{176}Lu/^{177}Hf$ ratios predicted for the SNC source regions is shown in gray, corresponding well to the majority of the magma ocean cumulates. The SNC source region predictions are compiled by *Borg and Draper* [2003].

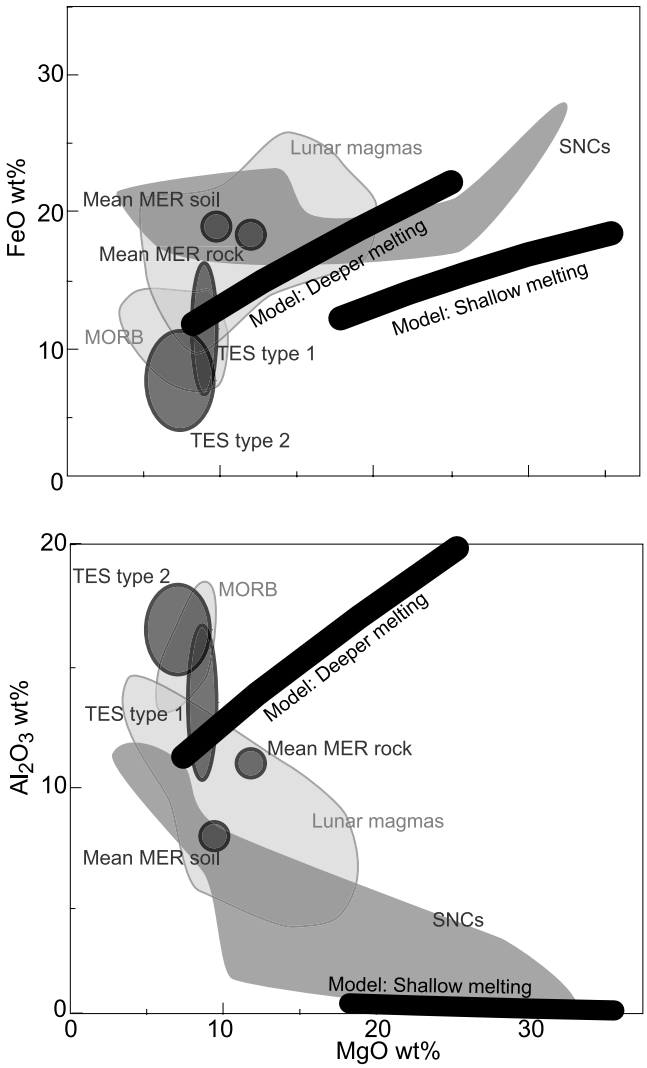

Figure 8. FeO and Al_2O_3 versus MgO wt% diagram showing the range of primary magmas predicted to form the ancient crust by this whole mantle magma ocean model (black) with the known SNC meteorite compositions, mean MER rock and soil, TES surface types 1 and 2 (gray), and other planetary data (MORBs: *Reynolds et al.* [1992] and *Reynolds and Langmuir* [1997]; lunar data: *Delano* [1986], *Elkins-Tanton et al.* [2003b], and *Papike et al.* [1998]; SNC meteorite compositions from *McSween and Treiman* [1998, and references therein], *Rubin et al.* [2000], *Taylor et al.* [2000], *Zipfel et al.* [2000], and *Barrat et al.* [2002]; TES surface type materials from *McSween et al.* [2003]; mean MER data compiled by *Nimmo and Tanaka* [2005]).

turn being an endogenic process capable of forming the crustal dichotomy. If magma extrusion occurs in a spherical harmonic degree-one pattern, this model predicts that the ancient, thick southern highland crust would be created from the shallower cumulate melting event during overturn, with a strikingly low-alumina, high Mg# basaltic composition from a source with an initial $^{147}Sm/^{144}Nd$ ratio near 0.20. The crust in the northern plains would be thinner, since it is produced from the deeper melting event with one-half the volume of the shallower event. The primary melt for the ancient crust of the northern plains would have an Mg# in the 70s, higher alumina, higher $^{147}Sm/^{144}Nd$, and higher silica than the southern plains, though in particular because of its depth of origin assimilation, fractionation, and mixing processes likely changed its composition on the way to the surface.

[39] The two compositions of early crust predicted in the whole mantle model are roughly consistent with Martian data for the northern and southern hemispheres. Data from the Thermal Emission Spectrometer (TES) aboard the Mars Global Surveyor [*Bandfield et al.*, 2000] has shown that the major element compositions of the southern highlands and the northern lowlands are significantly different. They find that basalts are concentrated in the south, and andesites in the north [*Nimmo and Tanaka*, 2005], consistent with the Mg#, alumina, and silica predictions from the models. Mars *Pathfinder* measured a rock with relatively high K_2O and SiO_2 (~57 wt%), perhaps an andesite [*Brückner et al.*, 2003]. The andesite characterization from remote sensing, however, remains controversial: the andesite signature may indicate weathering products or the presence of a large glass fraction in basalts. The TES surface type 1 [*McSween et al.*, 2003] is a closer fit to the magmas produced by the deeper melting event in our models (Figure 8) and is found in the northern lowlands, consistent with the hypothesis that the crustal dichotomy may be formed by endogenic magma ocean processes.

8. Conclusions

[40] Models of deep or complete magma oceans produce an earliest crust-forming event that consists of melts from two distinct source regions created during solid-state cumulate overturn to a gravitational stable stratigraphy. These melts are consistent with major and trace element data on SNCs and Martian crust from mission data as well as with volume estimates of crust from the northern and southern sides of the dichotomy. Shallower magma oceans eliminate the deeper melting source and produce an earliest crust from only the shallowest, olivine + pyroxene magmatic source. Magma oceans that are shallower still retain the shallowest melting region, but add the possibility of melt from primitive material that originated below the magma ocean but rose to melt during overturn.

[41] Though comparisons between modeled compositions and Martian data are favorable, these models make predictions of a specificity that can be tested in future missions. If melt from the two distinct source regions produced the crustal dichotomy, a possibility consistent with the volumes of melt predicted by the models, then the primary melts of the ancient crust in the northern lowlands should contain a far larger alumina content than the low-alumina, basaltic southern highlands. If a shallow magma ocean participated with primitive mantle material during overturn, then some fraction of melt from an undifferentiated source may exist in the most ancient crust. Predictions of melt volume also, when coupled with estimates for atmospheric opacity, allow calculation of the onset of the earliest conditions on Mars consistent with liquid surface water [*Sleep et al.*, 2001].

[42] **Acknowledgments.** This research is funded by a grant from the NASA Mars Fundamental Research Program. The authors thank Lars Borg and John Longhi for their thoughtful, constructive reviews.

References

Abe, Y. (1993), Physical state of very early Earth, *Lithos*, *30*, 223–235.

Abe, Y. (1997), Thermal and chemical evolution of the terrestrial magma ocean, *Phys. Earth Planet. Inter.*, *100*, 27–39.

Acuña, M. H., et al. (1999), Global distribution of crustal magnetization discovered by the Mars Global Surveyor MAG ER Experiment, *Science*, *284*, 790–793.

Agee, C. B., and D. S. Draper (2004), Experimental constraints on the origin of Martian meteorites and the composition of the Martian mantle, *Earth Planet. Sci. Lett.*, *224*, 415–429.

Anders, E., and N. Grevesse (1989), Abundances of the elements: Meteoritic and solar, *Geochim. Cosmochim. Acta*, *53*, 197–214.

Bandfield, J. L., V. E. Hamilton, and P. R. Christensen (2000), A global view of Martian surface compositions from MGS-TES, *Science*, *287*, 1626–1630.

Barrat, J. A., P. Gillet, V. Sautter, A. Jambon, M. Javoy, C. Gopel, M. Lesourd, F. Keller, and E. Petit (2002), Petrology and chemistry of the basaltic shergottite North West Africa 480, *Meteorit. Planet. Sci.*, *37*(4), 487–499.

Bertka, C. M., and Y. Fei (1997), Mineralogy of the Martian interior up to core-mantle boundary pressures, *J. Geophys. Res.*, *102*, 5251–5264.

Bertka, C. M., and Y. Fei (1998), Density profile of an SNC model Martian interior and the moment-of-inertia factor of Mars, *Earth Planet. Sci. Lett.*, *157*, 79–88.

Blichert-Toft, J., J. D. Gleason, P. Télouk, and F. Albarède (1999), The Lu-Hf geochemistry of shergottites and the evolution of the Martian mantle-crust system, *Earth Planet. Sci. Lett.*, *173*, 25–39.

Borg, L. E., and D. S. Draper (2003), A petrogenetic model for the origin and compositional variation of the Martian basaltic meteorites, *Meteorit. Planet. Sci.*, *38*, 1713–1731.

Borg, L. E., L. E. Nyquist, H. Wiesmann, and C.-Y. Shih (1997), Constraints on Martian differentiation processes from Rb-Sr and Sm-Nd isotopic analyses of the basaltic shergottite QUE 94201, *Geochim. Cosmochim. Acta*, *61*, 4915–4931.

Borg, L. E., L. E. Nyquist, H. Wiesmann, and Y. Reese (2002), Constraints on the petrogenesis of Martian meteorites from the Rb-Sr and Sm-Nd isotopic systematics of the lherzolitic shergottites ALH77005 and LEW88516, *Geochim. Cosmochim. Acta*, *66*, 2037–2053.

Boyet, M., and R. Carlson (2005), ^{142}Nd evidence for early (>4.53 Ga) global differentiation of the silicate Earth, *Science*, doi:10.1126/science.1113634.

Brandon, A. D., R. J. Walker, J. W. Morgan, and G. G. Goles (2000), Re-Os isotopic evidence for early differentiation of the Martian mantle, *Geochim. Cosmochim. Acta*, *64*, 4083–4095.

Brückner, J., G. Dreibus, R. Rieder, and H. Wänke (2003), Refined data of Alpha Proton X-ray Spectrometer analyses of soils and rocks at the Mars Pathfinder site: Implications for surface chemistry, *J. Geophys. Res.*, *108*(E12), 8094, doi:10.1029/2003JE002060.

Delano, J. W. (1986), Pristine lunar glasses: Criteria, data, and implications, *Proc. Lunar Planet. Sci. Conf. 16th*, Part 2, *J. Geophys. Res.*, *91*, suppl., D201–D213.

Draper, D. S., D. Xirouchakis, and C. B. Agee (2003), Trace element partitioning between garnet and chondritic melt from 5 to 9 Gpa: Implications for the onset of majorite transition in the Martian mantle, *Phys. Earth Planet. Inter.*, *139*, 149–169.

Elkins-Tanton, L. T., and E. M. Parmentier (2005), The fate of water in the Martian magma ocean and the formation of an early atmosphere, *Lunar Planet. Sci.*, *XXXVI*, abstract 1906.

Elkins-Tanton, L. T., E. M. Parmentier, and P. C. Hess (2003a), Magma ocean fractional crystallization and cumulate overturn in terrestrial planets: Implications for Mars, *Meteorit. Planet. Sci.*, *38*, 1753–1771.

Elkins-Tanton, L. T., N. Chatterjee, and T. L. Grove (2003b), Experimental and petrological constraints on lunar differentiation from the Apollo 15 green picritic glasses, *Meteorit. Planet. Sci.*, *38*, 515–527.

Elkins-Tanton, L. T., S. Zaranek, and E. M. Parmentier (2005), Early magnetic field and magmatic activity on Mars from magma ocean overturn, *Earth Planet. Sci. Lett.*, *236*, 1–12.

Frey, H. V., J. H. Roark, K. M. Shockey, E. L. Frey, and S. E. H. Sakimoto (2002), Ancient lowlands on Mars, *Geophys. Res. Lett.*, *29*(10), 1384, doi:10.1029/2001GL013832.

Ghiorso, M. S., and R. O. Sack (1995), Chemical mass transfer in magmatic processes. IV. A revised and internally consistent thermodynamic model for the interpolation and extrapolation of liquid-solid equilibria in magmatic systems at elevated temperatures and pressures, *Contrib. Mineral. Petrol.*, *119*, 197–212.

Green, T. H., J. D. Blundy, J. Adam, and G. M. Yaxley (2000), SIMS determination of trace element partition coefficients between garnet, clinopyroxene and hydrous basaltic liquids at 2–7.5 GPa and 1080–1200 degrees C, *Lithos*, *53*, 165–187.

Harper, C. L., Jr., L. E. Nyquist, B. Bansal, H. Weismann, and C.-Y. Shih (1995), Rapid accretion and early differentiation of Mars indicated by ^{142}Nd/^{144}Nd in SNC meteorites, *Science*, *267*, 213–217.

Hartman, W. K., and D. R. Davis (1975), Satellite-sized planetesimals and lunar origin, *Icarus*, *24*, 504–515.

Herd, C. D. K., L. E. Borg, J. H. Jones, and J. J. Papike (2002), Oxygen fugacity and geochemical variations in the Martian basalts: Implications for Martian basalt petrogenesis and the oxidation state of the upper mantle of Mars, *Geochim. Cosmochim. Acta*, *66*, 2025–2036.

Hess, P. C., and E. M. Parmentier (1995), A model for the thermal and chemical evolution of the Moon's interior: Implications for the onset of mare volcanism, *Earth Planet. Sci. Lett.*, *134*, 501–514.

Hess, P. C., and E. M. Parmentier (2001), Implications of magma ocean cumulate overturn for Mars, *Lunar Planet. Sci.*, *XXXII*, abstract 1319.

Jacobsen, S. B. (2005), The Hf-W isotopic system and the origin of the Earth and Moon, *Annu. Rev. Earth Planet. Sci.*, *33*, doi:10.1146/annurev.earth.33.092203.122614.

Jones, J. H. (1986), A discussion of isotopic systematics and mineral zoning in the shergottites: Evidence for a 180 m. y. igneous crystallization age, *Geochim. Cosmochim. Acta*, *50*, 969–977.

Kellogg, L. H., B. H. Hager, and R. D. van der Hilst (1999), Compositional stratification in the deep mantle, *Science*, *283*, 1881–1884.

Kleine, T., C. Munker, K. Mezger, and H. Palme (2002), Rapid accretion and early core formation on asteroids and the terrestrial planets from Hf-W chronometry, *Nature*, *418*, 952–955.

Longhi, J. (1991), Magmatic processes on Mars: Insights from SNC meteorites, *Lunar Planet. Sci.*, *XXI*, 716–717.

Longhi, J., E. Knittle, J. R. Holloway, and H. Wänke (1992), The bulk composition, mineralogy, and internal structure of Mars, in *Mars*, edited by H. H. Kieffer et al., pp. 184–208, Univ. of Ariz. Press, Tucson.

Martin, D., and R. Nokes (1989), A fluid-dynamic study of crystal settling in convecting magmas, *J. Petrol.*, *30*, 1471–1500.

McSween, H. Y., and A. H. Treiman (1998), Martian meteorites, in *Planetary Materials*, *Rev. Mineral.*, vol. 36, edited by J. J. Papike, pp. 6-1 to 6-53, Mineral. Soc. of Am., Washington, D. C.

McSween, H. Y., Jr., T. L. Grove, and M. B. Wyatt (2003), Constraints on the composition and petrogenesis of the Martian crust, *J. Geophys. Res.*, *108*(E12), 5135, doi:10.1029/2003JE002175.

Neumann, G. A., M. T. Zuber, M. A. Wieczorek, P. J. McGovern, F. G. Lemoine, and D. E. Smith (2004), Crustal structure of Mars from gravity and topography, *J. Geophys. Res.*, *109*, E08002, doi:10.1029/2004JE002262.

Nimmo, F., and K. Tanaka (2005), Early crustal evolution of Mars, *Annu. Rev. Earth Planet. Sci.*, *33*, doi:10.1146/annurev.earth.33.092203.122637.

Norman, M. D. (1999), The composition and thickness of the crust of Mars estimated from rare earth elements and neodymium-isotopic compositions of Martian meteorites, *Meteorit. Planet. Sci.*, *34*(3), 439–449.

Ohtani, E., K. Litasov, T. Hosoya, T. Kubo, and T. Kondo (2004), Water transport into the deep mantle and formation of a hydrous transition zone, *Phys. Earth Planet. Inter.*, *143–144*, 255–269.

Papike, J. J., G. Ryder, and C. K. Shearer (1998), Lunar samples, in *Planetary Materials*, *Rev. Mineral.*, vol. 36, edited by J. J. Papike, pp. 5-1 to 5-234, Mineral. Soc. of Am., Washington, D. C.

Purucker, M., D. Ravat, H. Frey, C. Voorhies, T. Sabaka, and M. Acuña (2000), An altitude-normalized magnetic map of Mars and its interpretation, *Geophys. Res. Lett.*, *27*, 2449–2452.

Reynolds, J. R., and C. H. Langmuir (1997), Petrological systematics of the Mid-Atlantic Ridge south of Kane: Implications for ocean crust formation, *J. Geophys. Res.*, *102*, 14,915–14,946.

Reynolds, J. R., C. H. Langmuir, J. F. Bender, K. A. Kastens, and W. B. F. Ryan (1992), Spatial and temporal variability of basalts from the East Pacific Rise, *Nature*, *359*, 493–499.

Ringwood, A. E., and S. E. Kesson (1976), A dynamic model for mare basalt petrogenesis, *Lunar Sci.*, *VII*, 1697–1722.

Rubin, A. E., P. H. Warren, J. P. Greenwood, R. S. Verish, L. Leshin, R. L. Hervig, R. N. Clayton, and T. K. Mayeda (2000), Los Angeles: The most differentiated basaltic Martian meteorite, *Geology*, *28*, 1001–1014, doi:10.1130/0091-7613.

Schubert, G., and T. Spohn (1990), Thermal history of Mars and the sulfur content of its core, *J. Geophys. Res.*, *95*, 14,095–14,104.

Shih, C.-Y., L. E. Nyquist, D. D. Bogard, G. A. McKay, J. L. Wooden, B. M. Bansai, and H. Weismann (1982), Chronology and petrogenesis of young achondrites, Shergotty, Zagami, and ALHA77005: Late magmatism on a geologically active planet, *Geochim. Cosmochim. Acta*, *46*, 2323–2344.

Shih, C.-Y., L. E. Nyquist, and H. Wiesmann (1999), Samarium-neodymium and rubidium-strontium systematics of nakhlite Governador Valadares, *Meteorit. Planet. Sci.*, *34*, 647–655.

Sleep, N. H., K. Zahnle, and P. S. Neuhoff (2001), Initiation of clement surface conditions on the earliest Earth, *Proc. Natl. Acad. Sci. U. S. A.*, *98*, 3666–3672.

Snyder, G. A., L. A. Taylor, and C. R. Neal (1992), A chemical model for generating the sources of mare basalts: Combined equilibrium and fractional crystallization of the lunar magmasphere, *Geochim. Cosmochim. Acta*, *56*, 3809–3823.

Solomatov, V. S. (2000), Fluid dynamics of a terrestrial magma ocean, in *Origin of the Earth and Moon*, edited by R. M. Canup and K. Righter, pp. 323–338, Univ. of Ariz. Press, Tucson.

Solomon, S. (1979), Formation, history, and energetics of cores in the terrestrial planets, *Phys. Earth Planet. Inter.*, *19*, 168–182.

Stevenson, D. J. (1990), Fluid dynamics of core formation, in *Origin of the Earth*, edited by N. E. Newsom and J. H. Jones, pp. 231–249, Oxford Univ. Press, New York.

Stolper, E. M., D. Walker, B. H. Hager, and J. F. Hays (1981), Melt segregation from partially molten source region: The importance of melt density and source region size, *J. Geophys. Res.*, *86*, 6261–6271.

Taylor, L. A., et al. (2000), Petrology of the Dhofar 019 shergottite, *Meteorit. Planet. Sci.*, *35*, suppl. S, A155.

Terasaki, H., D. C. Rubie, U. Mann, D. J. Frost, and F. Langenhorst (2005), The effects of oxygen, sulfur, and silicon on the dihedral angles between Fe-rich liquid metal and olivine, ringwoodite, and silicate perovskite: Implications for planetary core formation, *Lunar Planet. Sci.*, *XXXVI*, abstract 1129.

Tonks, W. B., and H. J. Melosh (1990), The physics of crystal settling and suspension in a turbulent magma ocean, in *Origin of the Earth*, edited by N. E. Newsom and J. H. Jones, pp. 151–174, Oxford Univ. Press, New York.

Walker, D., and W. S. Kiefer (1985), Xenolith digestion in large magma bodies, *Proc. Lunar Planet. Sci. Conf. 15th*, Part 2, *J. Geophys. Res.*, *90*, suppl., C585–C590.

Warren, P. H. (1985), The magma ocean concept and lunar evolution, *Annu. Rev. Earth Planet. Sci.*, *13*, 201–240.

Wetherill, G. W. (1990), Formation of the Earth, *Annu. Rev. Earth Planet. Sci.*, *18*, 205–256.

Wetherill, G. W., and S. Inaba (2000), Planetary accumulation with a continuous supply of planetesimals, *Space Sci. Rev.*, *92*, 311–320.

Wood, J. A., J. S. Dickey, U. B. Marvin, and B. N. Powell (1970), Lunar anorthosites and a geophysical model of the moon, in *Proceedings of the Apollo 11 Science Conference*, pp. 965–988, Elsevier, New York.

Yin, Q., S. Jacobsen, K. Yamashita, J. Blichert-Toft, P. Telouk, and F. Albarede (2002), A short timescale for terrestrial planet formation from Hf-W chronometry of meteorites, *Nature*, *418*, 949–952.

Zaranek, S. E., and E. M. Parmentier (2004), Convective cooling of an initially stably stratified fluid with temperature-dependent viscosity: Implications for the role of solid-state convection in planetary evolution, *J. Geophys. Res.*, *109*, B03409, doi:10.1029/2003JB002462.

Zaranek, S., L. T. Elkins-Tanton, and E. Parmentier (2004), Magma ocean overturn: Implications for the creation of large scale mantle heterogeneities and influences on planetary evolution, *Eos Trans. AGU*, *85*(47), Fall Meet. Suppl., Abstract P33A-1010.

Zhong, S.-J., and M. T. Zuber (2001), Degree-1 mantle convection and the crustal dichotomy on Mars, *Earth Planet Sci. Lett.*, *189*, 75–84.

Zipfel, J., P. Scherer, B. Spettel, G. Dreibus, and L. Schultz (2000), Petrology and chemistry of the new shergottite Dar al Gani 476, *Meteorit. Planet. Sci.*, *35*, 95–106.

L. T. Elkins-Tanton, P. C. Hess, and E. M. Parmentier, Department of Geological Sciences, Brown University, 324 Brook Street, Providence, RI 02912, USA. (linda_elkins_tanton@brown.edu)